Dynamics of biexciton localization in $Al_xGa_{1-x}N$ mixed crystals under exciton resonant excitation

Daisuke Hirano,[1] Takeshi Tayagaki,[1] Yoichi Yamada,[2] and Yoshihiko Kanemitsu[1,3,*]
[1]*Institute for Chemical Research, Kyoto University, Uji, Kyoto 611-0011, Japan*
[2]*Department of Electrical and Electronic Engineering, Yamaguchi University, Ube, Yamaguchi 755-8611, Japan*
[3]*Photonics and Electronics Science and Engineering Center, Kyoto University, Kyoto 615-8510, Japan*
(Received 18 March 2008; published 30 May 2008)

We report the localization dynamics of biexcitons in $Al_xGa_{1-x}N$ mixed crystals under exciton resonant excitation at low temperatures. During a few tens of picoseconds just after intense laser excitation, the photoluminescence (PL) spectral shape obeys an inverse Maxwell–Boltzmann distribution and free biexcitons dominate the PL spectrum. With a further increase in the delay time, the biexciton PL peak energy and edge energy shift to lower energies. These redshift behaviors in $Al_xGa_{1-x}N$ mixed crystals are completely different from the behaviors of free biexcitons in GaN crystals. Our observations reveal the rapid transformation dynamics from free to localized biexcitons in band-tail states in $Al_xGa_{1-x}N$ mixed crystals.

DOI: 10.1103/PhysRevB.77.193203 PACS number(s): 78.55.Cr, 78.47.Cd, 71.35.−y

In semiconductor mixed crystals such as $Al_xGa_{1-x}N$ and $In_xGa_{1-x}N$, alloy disorders are induced by random fluctuations in the composition x, and these disorders cause the formation of localized, so-called "band-tail," states below the band edge.[1] Excitons are localized in the band tail, which are observed as line broadening in the optical transitions around the band edge.[2,3] The localized excitons determine the optical properties of the mixed crystals.[2–9] Furthermore, the localized band-tail states play an essential role in excitonic many-body effects under high excitation conditions, such as excitonic optical gain[10–12] and the formation of biexcitons (excitonic molecules).[6–8] The biexcitons are localized in the band-tail states, similar to the case of excitons. However, the dynamic aspects of the transformation from free to localized biexcitons and the relaxation of biexcitons into localized band-tail states are not clear.

Due to the very small exciton Bohr radii in wide-gap GaN-based mixed crystals, their optical properties are very sensitive to spatial potential fluctuations.[13–16] Then, $Al_xGa_{1-x}N$ mixed crystals make an excellent sample for the study of exciton-related luminescence and the localization dynamics of excitons and biexcitons in semiconductors. Moreover, studies on the dynamics of localized excitons and biexcitons in highly excited $Al_xGa_{1-x}N$ mixed crystals are needed to clarify fundamental excitonic processes and lasing mechanisms in wide-gap semiconductors.[10–12,15]

In this Brief Report, we investigated the time-resolved photoluminescence (PL) spectra of highly excited $Al_xGa_{1-x}N$ mixed crystals and the dynamics of biexciton localization in band-tail states. Under exciton resonant excitation, the spectral shape of the biexciton luminescence obeys an inverse Maxwell–Boltzmann distribution for 20 ps or less. This behavior is similar to that of free biexcitons in GaN. After several tens of picoseconds, however, the redshift of the PL energy and the edge energy of biexcitons evolve with time, signifying the transformation from free to localized biexcitons in the $Al_xGa_{1-x}N$ mixed crystals.

The samples were $Al_xGa_{1-x}N$ and GaN epitaxial films. Following the deposition of GaN buffer layers, 1-μm-thick $Al_xGa_{1-x}N$ epitaxial layers were grown on (0001) sapphire substrates using a metalorganic chemical vapor deposition technique.[14] The $Al_xGa_{1-x}N$ epitaxial layers examined in this study had aluminum concentrations of $x=0.038$, 0.057, and 0.077.

Wavelength-tunable femtosecond laser pulses, obtained from an optical parametric amplifier system based on a regenerative amplified Ti:sapphire laser, were used as the excitation source. The excitation energy was set at the free exciton energy for each sample. The pulse duration and the repetition rate were ~150 fs and 1 kHz, respectively. The sample temperature was kept at 7 K and the typical laser spot size on the samples was 100 μm. An optical Kerr gate method in a 1-mm-thick quartz cell having toluene as the Kerr medium was used for the time-resolved PL spectral measurements with a time resolution of 0.7 ps. The PL spectra were measured as a function of delay time using a liquid-nitrogen-cooled charge coupled device with a 50-cm single monochromator.

The inset of Fig. 1 shows the time-integrated PL spectrum under an excitation intensity of 7 $\mu J/cm^2$. The excitation energy was tuned to the band-to-band excitation of 3.761 eV.

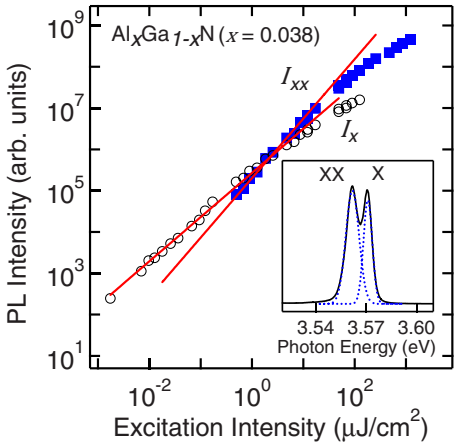

FIG. 1. (Color online) Exciton (I_X) and biexciton (I_{XX}) PL intensities in $Al_xGa_{1-x}N$ ($x=0.038$) as a function of excitation intensity. The solid lines show power law fitting results. Inset: Time-integrated localized exciton and biexciton PL spectra at an excitation intensity of 7 $\mu J/cm^2$. The dotted line indicates the fitting result of applying two Gaussian functions.

 ©2008 The American Physical Society

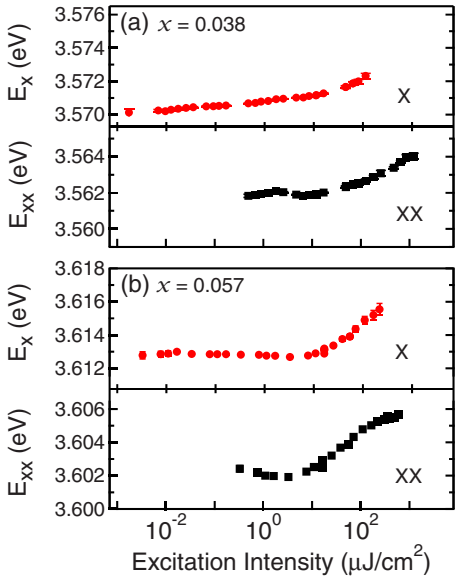

FIG. 2. (Color online) PL peak energies of excitons (E_X) and biexcitons (E_{XX}) as a function of the excitation intensity in the $Al_xGa_{1-x}N$ samples with (a) $x=0.038$ and (b) $x=0.057$.

Double PL peaks are clearly observed in the medium intensity range between 0.1 and 100 $\mu J/cm^2$. In our $Al_xGa_{1-x}N$ mixed crystal samples, there are Stokes shifts between the PL and PL excitation peaks in the exciton and biexciton spectra.[17] These two time-integrated PL spectra peaks are assigned to the localized excitons (X) and the localized biexcitons (XX).[17] As shown by the blue dotted curves, we evaluate the PL intensities and peak energies of the localized excitons and biexcitons using two Gaussian functions.

Figure 1 shows the time-integrated PL intensity of excitons (I_X) and biexcitons (I_{XX}) in $Al_xGa_{1-x}N$ ($x=0.038$) as a function of the excitation laser intensity (I_{laser}). As shown by the solid red lines, the exciton and biexciton PLs show linear and superlinear intensity dependences. The excitation intensity dependence of the biexciton PL is approximately given by $I_{xx} \propto I_{laser}^{1.4}$. This small power index is due to a short biexciton lifetime.[18] In contrast, both intensities, I_X and I_{XX} show saturation at excitation intensities higher than 20 $\mu J/cm^2$.

In Fig. 2, the PL peak energies of the localized excitons (E_X) and biexcitons (E_{XX}) are plotted as a function of excitation intensity for the $Al_xGa_{1-x}N$ samples of (a) $x=0.038$ and (b) $x=0.057$. While the peak positions are almost unchanged under weak excitation (<10 $\mu J/cm^2$), under intense excitation, E_X and E_{XX} simultaneously blueshift with PL intensity saturation. This excitation intensity dependence of the peak shifts and the PL intensities are observed in all the $Al_xGa_{1-x}N$ ($x=0.038$, 0.057, and 0.077) samples. These phenomena in $Al_xGa_{1-x}N$ mixed crystals are explained by the state-filling effects of the band-tail states,[10–12] that is, the saturation of the localized states and the population transfer to the delocalized states under high laser excitation. While excitons and biexcitons appear at localized states under weak excitation, filling of the localized states under high-intensity excitation causes a rise in the effective temperature in excitonic systems and a redistribution to delocalized states. Note that the behavior of biexcitons is very similar to that of excitons.

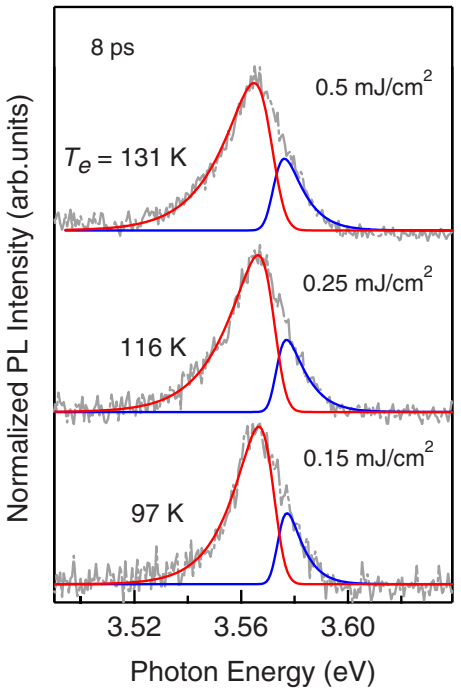

FIG. 3. (Color online) Time-resolved PL spectra measured at 8 ps delay in the $Al_xGa_{1-x}N$ ($x=0.038$) sample under different excitation intensities: (a) 0.5 mJ/cm^2, (b) 0.25 mJ/cm^2, and (c) 0.15 mJ/cm^2. The solid lines show the fitting results for free biexcitons and excitons. T_e represents the effective biexciton temperatures obtained by fitting.

To clarify the transformation from free to localized biexcitons and the relaxation dynamics of localized biexcitons in the band-tail state, we performed time-resolved PL measurements. Figure 3 shows the PL spectra of the $Al_xGa_{1-x}N$ ($x=0.038$) sample at 8 ps time delay under 3.581 eV excitation at different intensities. With an increase in excitation intensity, the PL spectral shape becomes broad and asymmetric, and the lower-energy tail of the PL spectrum grows.

In the radiative annihilation of biexcitons, a biexciton (an excitonic molecule) changes into a free exciton and a photon. The free biexciton PL spectrum has an asymmetric line shape with a low-energy tail, and the PL spectral shape is well described by the inverse Maxwell–Boltzmann distribution function.[19] In the spectral analysis, the inhomogeneous broadening is taken into account by convoluting the inverse Maxwell–Boltzmann distribution function with a Lorentzian function,[20]

$$I(\hbar\omega_m) \propto \int \frac{[E_0-\varepsilon]^{1/2}\exp[-(E_0-\varepsilon)/k_BT]\Gamma}{(\hbar\omega_m-\varepsilon)^2+\Gamma^2}d\varepsilon, \quad (1)$$

where E_0 is the edge energy of the biexciton luminescence, and Γ is an inhomogenous broadening parameter depending on the composition x. The PL intensity $I(\hbar\omega_m)$ is proportional to the density of the thermalized biexcitons (the Maxwell–Boltzmann distribution) and therefore, the PL spectral shape is given by the above inverse Maxwell–Boltzmann distribution function. On the other hand, the PL spectrum shape of free excitons has a higher energy tail and

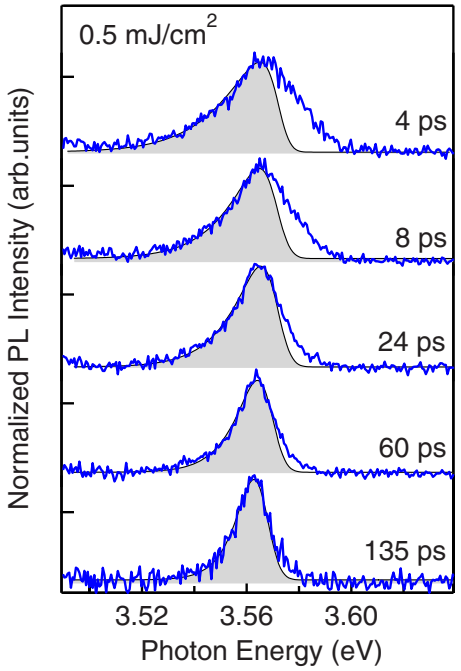

FIG. 4. (Color online) Time-resolved PL spectra of the $Al_xGa_{1-x}N$ ($x=0.038$) sample at an excitation intensity of 0.5 mJ/cm^2. The hatched areas indicate the fitting results for biexcitons using the inverse Maxwell–Boltzmann distribution.

is described by the Maxwell–Boltzmann distribution. In the exciton PL spectral fitting, we use the Maxwell–Boltzmann distribution function with a Lorentzian broadening. We assume that the early stage time-resolved PL originates from free excitons and free biexcitons, and so we deconvoluted the PL spectra into two components using the fitting model including free excitons and biexcitons. In the spectral fitting of the $x=0.038$ sample shown in Fig. 3, we used $\Gamma=3$ and 5 meV and free edge energies $E_0=3.581$ and 3.571 eV for excitons and biexcitons, respectively, where the biexciton binding energy is 10 meV.[14,17] This early stage PL spectral shape is well described by the above-mentioned model for excitons and biexcitons. Under exciton resonant excitation, the effective temperature of biexcitons, T_e, increases with the excitation intensity as shown in Fig. 3. Hereafter, we focus on the temporal evolution of the biexciton dynamics under high-intensity excitation.

Figure 4 shows the time-resolved PL spectra of $Al_xGa_{1-x}N$ ($x=0.038$) under 0.5 mJ/cm^2 excitation. At 4 ps delay, a broad PL spectrum peaked at 3.565 eV appears. At an early stage, the spectral shape of biexciton luminescence obeys an inverse Maxwell–Boltzmann distribution function (hatched area in Fig. 4) indicating the existence of free biexcitons in $Al_xGa_{1-x}N$ for a few tens of picoseconds. With time evolution, the spectral shapes show redshift and become narrow, and the biexcitons are localized into the lower-energy band-tail state. After about 100 ps delay, the emission peak energy becomes independent of time and the spectral shape becomes symmetrical, indicating the localization of the biexcitons into the lower-energy band-tail states.

In mixed crystals, variations of the binding energy and localization energy of biexcitons lead to the spectral broadening. The PL spectral shape reflects the energy profiles of the localized state and the thermal distribution of the biexcitons. The origin of the broad PL spectra and the spectral shape analysis during the transformation from free to localized biexciton are complicated. For simplicity, we use Eq. (1) including the spectral broadening, in order to analyze and discuss the essential features of the biexciton PL spectra. We obtain the biexciton PL peak energy E_{PL}, the edge energy E_0, and the effective temperature T_e, from the biexciton spectral fitting of the time-resolved PL spectra.

Figure 5(a) shows the temporal change of E_{PL}, E_0, and T_e in the $Al_xGa_{1-x}N$ ($x=0.038$) sample under 0.5 mJ/cm^2 excitation. For comparison, the temporal change of E_{PL}, E_0, and T_e in the GaN crystal under 0.5 mJ/cm^2 excitation is summarized in Fig. 5(b). Note that the two parameters, T_e and E_0, determine the biexciton PL spectral shape.

As shown in Fig. 5(a), the dynamic behavior of biexcitons at short delay times (<20 ps) is different from those at longer delay times. Although the blueshift of the PL peak energy E_{PL} occurs at delay times of less than 20 ps, the edge energy, E_0, remains almost constant. This temporal behavior is very similar to that of free biexcitons in the GaN sample. For the free biexcitons in Fig. 5(b), the peak energy E_{PL} increases with a decrease in T_e, and the time-independent

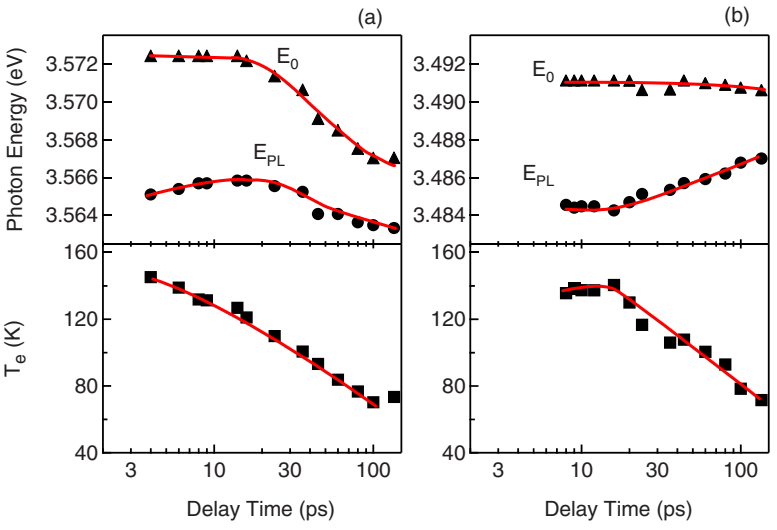

FIG. 5. (Color online) Temporal evolution of the peak energy E_{PL}, the edge energy E_0, and the effective biexcitons temperature T_e in the $Al_xGa_{1-x}N$ ($x=0.038$) (a) and GaN samples (b). The solid curves are visual guides.

edge energy E_0 corresponds to the well-defined lowest energy of the free biexciton at $k=0$. Even in the $Al_xGa_{1-x}N$ ($x=0.038$) sample during the early stage, the biexciton temperature is higher than 100 K and the free biexciton luminescence dominates the PL spectrum. Similar behavior is observed only under excitations higher than 0.2 mJ/cm^2.

After a 20 ps time delay, however, the edge energy E_0 becomes time-dependent. Note that both the peak energy E_{PL} and the edge emission energy E_0 show redshift in the long time delay region. These behaviors are different from the free biexciton behavior in GaN. The E_0 redshift in $Al_xGa_{1-x}N$ mixed crystals suggests the appearance of localized biexcitons in the band-tail states. Since the radiative annihilation of localized biexcitons is caused by the transition from localized biexciton states to free excitons, and not to localized excitons, the edge energy E_0 is indicative of the lowest energy of biexcitons. The energy difference between the time-independent E_0 of the free biexcitons and the time-dependent E_0 of the localized biexcitons corresponds to the localization energy of the biexcitons E_{loc}. The effective temperature T_e is comparable to the localization energy of the biexcitons, $E_{loc}=5$ meV at 100 ps delay, and to the inhomogeneous broadening of the biexcitons, $\Gamma=5$ meV. Therefore, even after E_0 starts to redshift, the spectral shape is approximately described by inverse Maxwell–Boltzmann distribution functions. After the biexcitons are relaxed into the lower-energy state, the PL spectrum reflects the energy distribution of the thermalized biexcitons in the localized states. We conclude that the edge energy E_0 is the most reliable parameter for judging the localization of biexcitons. Our subpicosecond time-resolved PL measurements under exciton resonant excitation can reveal the free biexciton state and the localization dynamics of biexcitons in $Al_xGa_{1-x}N$ mixed crystals.

In conclusion, we report the first observation of free biexcitons and transformation dynamics from free to localized biexcitons in $Al_xGa_{1-x}N$ mixed crystals. Under intense exciton resonant excitation, we observed that asymmetric spectra were described by the inverse Maxwell–Boltzmann distribution function. We further observed that free biexcitons exist during the first few tens of picoseconds, followed by the rapid localization of biexcitons. Our findings reveal the rapid localization of biexcitons in GaN-based mixed crystals.

Part of this study was supported by a Grant-in-Aid for Scientific Research from the Japan Society for the Promotion of Science and the Global Center of Excellence (G-COE) program from MEXT.

*Corresponding author; kanemitu@scl.kyoto-u.ac.jp

[1] See, for example, N. F. Mott and E. A. Davis, *Electronic Processes in Non-Crystalline Materials* (Oxford University, Oxford, 1979).
[2] E. Cohen and M. D. Sturge, Phys. Rev. B **25**, 3828 (1982).
[3] S. Permogorov, A. Rentitskii, S. Verbin, G. O. Müller, P. Flögel, and M. Nikiforova, Phys. Status Solidi B **113**, 589 (1982).
[4] G. Noll, U. Siegner, S. G. Shevel, and E. O. Göbel, Phys. Rev. Lett. **64**, 792 (1990).
[5] H. Schwab, V. G. Lyssenko, J. M. Hvam, and C. Klingshirn, Phys. Rev. B **44**, 3413 (1991).
[6] J. Y. Bigot, A. Daunois, J. Oberlé, and J. C. Merle, Phys. Rev. Lett. **71**, 1820 (1993).
[7] W. Langbein, J. M. Hvam, M. Umlauff, H. Kalt, B. Jobst, and D. Hommel, Phys. Rev. B **55**, R7383 (1997).
[8] W. Langbein and J. M. Hvam, Phys. Rev. B **59**, 15405 (1999).
[9] Y. Kanemitsu, K. Tomita, D. Hirano, and H. Inouye, Appl. Phys. Lett. **88**, 121113 (2006).
[10] J. Ding, H. Jeon, T. Ishihara, M. Hagerott, A. V. Nurmikko, H. Luo, N. Samarth, and J. Furdyna, Phys. Rev. Lett. **69**, 1707 (1992).
[11] Y. Yamada, Y. Masumoto, T. Mullins, and T. Taguchi, Appl. Phys. Lett. **61**, 2190 (1992).
[12] A. Satake, Y. Masumoto, T. Miyajima, T. Asatsuma, and M. Ikeda, Phys. Rev. B **60**, 16660 (1999).
[13] G. Coli, K. K. Bajaj, J. Li, J. Y. Lin, and H. X. Jiang, Appl. Phys. Lett. **78**, 1829 (2001).
[14] Y. Yamada, Y. Ueki, K. Nakamura, T. Taguchi, A. Ishibashi, Y. Kawaguchi, and T. Yokogawa, Appl. Phys. Lett. **84**, 2082 (2004).
[15] D. Hirano, T. Tayagaki, and Y. Kanemitsu, Phys. Rev. B **77**, 073201 (2008).
[16] F. S. Cheregi, A. Vinattieri, E. Feltin, D. Simeonov, J. F. Carlin, R. Butté, N. Grandjean, and M. Gurioli, Phys. Rev. B **77**, 125342 (2008).
[17] Y. Yamada, Y. Ueki, K. Nakamura, T. Taguchi, A. Ishibashi, Y. Kawaguchi, and T. Yokogawa, Phys. Rev. B **70**, 195210 (2004).
[18] R. T. Phillips, D. J. Lovering, G. J. Denton, and G. W. Smith, Phys. Rev. B **45**, 4308 (1992).
[19] M. Ueda, H. Kanzaki, K. Kobayashi, Y. Toyozawa, and E. Hanamura, *Excitonic Processes in Solids* (Springer, Berlin, 1986).
[20] S. Shionoya, H. Saito, E. Hanamura, and O. Akimoto, Solid State Commun. **12**, 223 (1973).